PCCP

PERSPECTIVE

View Article Online
View Journal | View Issue

Cite this: *Phys. Chem. Chem. Phys.*, 2025, **27**, 6400

Platinum-based nanoalloys for the oxygen reduction reaction: exposing the true active phase *via in situ/operando* techniques

Carlos A. Campos-Roldán, * Raphaël Chattot, Pierre-Yves Blanchard, Deborah J. Jones and Sara Cavaliere *

Received 22nd September 2024,
Accepted 21st February 2025

DOI: 10.1039/d4cp03665d

rsc.li/pccp

Platinum-based nanoalloys are efficient electrocatalysts for the oxygen reduction reaction (ORR). *In situ/operando* measurements have revealed that key properties including induced strain, chemical composition, coordination environment, evolve significantly during operation, which can hampertheir effective implementation in fuel cells. In fact, recent studies indicate that the impact of the early surface activation steps of Pt-based nanoalloys has been hitherto underestimated and is an important factor contributing to loss of their initial electroactivity. In this short perspective, we highlight the importance of *in situ/operando* characterization of Pt-based electrocatalysts during the initial operation steps in the ORR and discuss recent insights into their early degradation and evolution of their key properties during electrochemical characterization.

Introduction

The current interest in fuel cells (FCs) and electrolyzers stems from the versatility of hydrogen in sector coupling and its contribution to the transition to CO_2 emission neutrality.[1] Nevertheless, technical bottlenecks still remain,[2,3] in particular

ICGM, Univ. Montpellier, CNRS, ENSCM, 34095 Montpellier, cedex 5, France. E-mail: carlos-augusto.campos-roldan@umontpellier.fr, sara.cavaliere@umontpellier.fr

Carlos A. Campos-Roldán

Carlos Augusto Campos-Roldán received his PhD degree in 2020 under collaboration between ESIQIE-IPN, Mexico, and the University of Poitiers, France. His thesis was awarded in 2020 as the best electrochemistry thesis in the 13th meeting of the Mexican Section of the International Society of Electrochemistry. Currently, he is a postdoc at the University of Montpellier, France. His research interests relay on the design and understanding of nano-structured electrocatalysts for fuel cells and electrolyzers.

Raphaël Chattot

Raphaël Chattot earned his PhD in Electrocatalysis from the University of Grenoble-Alpes in 2017. Following a postdoctoral fellowship shared between the Laboratory of Electrochemistry and Physicochemistry of Materials and Interfaces (LEPMI, Grenoble, France) and the European Synchrotron Radiation Facility (ESRF, Grenoble, France), he became a Junior Scientist at the ESRF's ID31 beamline. Since 2021, he has been a permanent researcher at the French National Center for Scientific Research (CNRS), based at the Institute Charles Gerhardt (ICGM) in Montpellier, France. His research emphasizes the investigation of the fundamental role of nanoscale structural disorder in electrocatalysis for energy conversion systems, such as fuel cells and water electrolyzers, using advanced in situ and operando X-ray scattering techniques.

the catalyst layer at the cathode of proton exchange membrane fuel cells (PEMFC),[4] which requires a high Pt loading to drive the sluggish oxygen reduction reaction (ORR). The rational design of highly active and long-term stable Pt-based electrocatalysts for the ORR is, therefore, a research field of paramount importance, to reach industry targets of 0.1 g_{PGM} kW^{-1} (platinum-group metal, PGM) for automotive and 0.3 g_{PGM} kW^{-1} for heavy-duty transport applications.[5] Within this context, exhaustive research has resulted in strong increase of the ORR activity, as determined using the thin-film rotating disk electrode (RDE) technique, by alloying Pt with late transition metals (usually Ni, Co, Fe, Cu, *etc.*), which also decreases simultaneously the amount of Pt.[4] The RDE technique characterizes a half-cell reaction of a fuel cell in an idealized environment, and allows determination of the intrinsic ORR activity *via* the kinetic current evaluated at a given electrode potential (usually at 0.9 V_{RHE}). However, strong discrepancy is frequently observed between the activity observed in the RDE and that in a PEMFC.[6] Bridging the gap between these *ex situ* and *in situ* electrochemical results is crucial to advancing understanding of novel Pt-based nanostructures as PEMFC electrocatalysts. Along with the control of electrode structure,[7] this calls for characterization of how key properties of the electrocatalysts evolve *e.g.*, in terms of atomic-scale structure and surface chemistry under operation conditions to understand any loss in electrocatalytic activity and stability. In this context, *in situ*/*operando* characterization techniques play a crucial role in understanding the relationship between structure, activity, and stability in electrochemical environments. These methods not only allow the identification of the active phase in the system, often differing from that observed in *ex situ* studies, but also enable real-time tracking of structural changes during electrocatalyst operation.

The development of *in situ* and/or *operando* techniques, such as X-ray diffraction/scattering (XRD),[8] X-ray absorption spectroscopy (XAS),[9,10] online inductively coupled plasma – mass spectrometry (ICP-MS),[11] liquid phase electron microscopy,[12,13] *etc.* has allowed better understanding of electrocatalyst behavior in real conditions or electrochemical environments simulating those of the application device. The fundamentals advances of each technique are reviewed in the corresponding cited papers.

Quasi *in situ* techniques, such as identical-location transmission-electron microscopy (IL-TEM) coupled with advanced detectors and automatization approaches are also powerful tools to investigate structure–activity–stability relationships in Pt-based ORR catalysts.[14,15] Insights from use of these *in situ*/*operando* techniques have revealed inevitable catalyst surface reconstruction in the particular environment of the PEMFC cathode on operation,[9,16] and shown that the largely accepted fundamental reactivity descriptors (*e.g.*, ligand, strain, and ensemble effects) of Pt-based electrocatalysts tailored and measured *ex situ* are not fully conserved *in situ*.[17] These structural and activity changes can be so significant, that the as-synthesized materials have been referred to as "pre-catalysts" under non-reaction conditions, while the restructured components in actual reaction conditions are the "catalysts".[18,19] With the impressive development of modern *in situ*/*operando* techniques, few contributions (mainly recent, apart from that in 2013[20]) have considered the role of the electrochemical activation steps on the catalyst properties. Within this context, it is of

Pierre-Yves Blanchard

Pierre-Yves Blanchard is assistant professor in chemistry at University of Montpellier (France) since 2017. His current research focuses on the development of proton exchange membrane fuel cell and chemically regenerative redox fuel cells. He received his PhD at the University of Angers (France) in 2013 on surface modification and electrochemical characterization. His current interest is to develop ex situ and in situ analytical techniques coupled with electrochemistry for energy devices.

Deborah J. Jones

Deborah Jones received her PhD from the University of London, King's College. She is CNRS Research Director Emeritus at the Institute for Molecular Chemistry and Materials, ICGM, Montpellier. Her interests encompass the development and operando characterisation of hydrogen energy materials for proton and anion exchange membrane fuel cells and electrolysers.

Sara Cavaliere

Sara Cavaliere is Full Professor of Chemistry at the University of Montpellier (France) Institute Charles Gerhardt Montpellier (ICGM). She received her PhD in Chemistry and Materials Science in 2006 from the University of Versailles Saint-Quentin-en-Yvelines, France, after graduating in Chemistry from University of Milan, Italy. Her research interests focus on design, synthesis and characterization of nanostructured core materials for low temperature ion exchange membrane fuel cells and electrolyzers.

paramount importance to encourage the community to consider this emerging topic to improve understanding of mechanisms of reaction and degradation in electrocatalysis.

In this short perspective, we highlight the systematic need for *in situ/operando* characterization of Pt-based nanoalloys to unravel their structural self-reconstruction bridging precatalysts with true catalysts. We also discuss recent results and provide insights to the early degradation of Pt-based nanoalloys prior to ORR, which is critical for unambiguous evaluation of the intrinsic properties of the electrocatalysts.

In situ/operando characterization techniques

Fundamental understanding of the property–activity–stability relationships in electrocatalysis is crucial to the tailoring of advanced nanostructured materials for the electrochemical reactions of energy conversion devices, such as fuel cells and electrolyzers. *Ex situ* characterization of the electrocatalyst state before and after a specific reaction (*e.g.*, ORR) is the most common method to deduce possible active sites or activity/stability descriptors. Nevertheless, stepwise reaction kinetics, structural/compositional transitions through surface reconstruction, the presence of short-lived reaction intermediates, *etc.*, are clearly undetectable by *ex situ* techniques. Fig. 1 sketches the main properties of Pt-based nanostructures susceptible to evolve during the electrode manufacturing and/or the electrochemical operating steps, which are not captured by *ex situ* characterization techniques performed at the catalyst synthesis stage.

In situ/operando characterization techniques offer the possibility of probing electrocatalyst–reactant interactions over multiple length scales (depending on the technique used and its inherent limitations, see Fig. 2), but most importantly, over all different steps of catalysts life. For instance, electrocatalyst crystalline structure (atomic long-range ordering), and the local electronic structure and coordination environment of the probe element may be elucidated by *in situ/operando* XRD and XAS, respectively. Synchrotron radiation is therefore needed for high flux and tunable energy and brilliance of the X-rays produced.[21] Furthermore, their highly penetrating properties allow the investigation of the electrocatalysts in liquid–electrolyte and solid–electrolyte fuel cells under operation.[22,23]

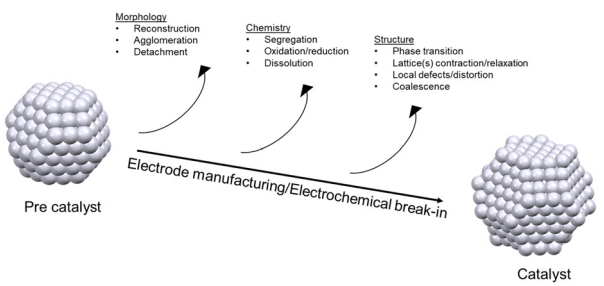

Fig. 1 Schematic representation of the main properties susceptible to change according to various mechanisms during the transformation of an as-prepared material (precatalyst) to that in an operating electrode.

Besides, the evolution of the electrocatalyst morphology can be observed (under certain limitations)[12] by *in situ* liquid cell transmission electron microscopy (TEM).[12,13] Complementarily, *in situ/operando* vibrational spectroscopic techniques (*e.g.*, Fourier-transform infrared spectroscopy-FT-IR-, and Raman spectroscopy) have been applied in electrocatalysis research to track the formation/consumption of adsorbed intermediates at the electrode–electrolyte interface.[24] Furthermore, electrocatalyst degradation can be probed by online detection of the species dissolved into the electrolyte by mass spectrometry (online ICP-MS).[25] The latter was mostly restricted to liquid electrolyte environment but has been recently adapted to investigate electrocatalyst in gas diffusion electrode half-cell, possibly with polymeric electrolyte.[26]

Within this context and as it is shown in Fig. 1, *in situ/operando* techniques have clearly revealed that electrocatalyst properties undergo dynamic evolution during electrochemical operating conditions. Namely, the morphology (surface reconstruction and possible particle agglomeration/detachment), chemical composition (alloy segregation and dissolution) and structure (crystalline phase transitions, lattice contraction/relaxation, changes in local coordination) differ within the operating environment relative to the precatalysts. This evolution/degradation mechanism, however, is rather complex and it is dominated by several factors. Therefore, in-depth understanding of the corresponding property–activity–stability relationships through use of only a single *in situ/operando* approach is difficult,[27] since each technique is specific to a length scale (specific probing mechanism/region). For instance, while high-energy X-ray and electron-based techniques can probe the bulk structure of the electrode, low-energy vibrational spectroscopies can provide insights regarding the electrode/electrolyte interface, and analysis of the electrolyte gives important information concerning catalyst dissolution, see Fig. 2. Moreover, each technique presents its own specific limitations, and thus provides information from within its specific scope (temporal/spatial resolution, detection limit, detection interferences, *etc.*). Combining information extracted from more than one *in situ/operando* technique and complementary approaches (*e.g.*, *ex situ* characterizations, DFT calculations) can provide a reliable picture of property–activity–stability relationships. Indeed, since the ORR could be described by Sabatier's principle (activity volcano plots), combining *in situ/operando* measurements with high throughput machine learning-assisted theoretical calculations might provide an intuitive guide to catalyst design.

The electrochemical testing protocol of an ORR electrocatalyst usually starts with surface conditioning, *i.e.*, electrochemical activation (ECA), to remove any surface contaminants and reach a defined initial surface state. The ECA significantly contributes to self-reconstruction of the electrocatalyst surface, with not insignificant impact on activity and stability of Pt-based nanoalloys. However, this process is often under-investigated and electrocatalytic performance attributed to the precatalyst characteristics. Although the properties determined *in situ* describe the beginning of life state of the electrocatalyst, detailed study of the evolution of properties of Pt-based nanoalloys during the ECA is rare. Hereafter we will discuss recent

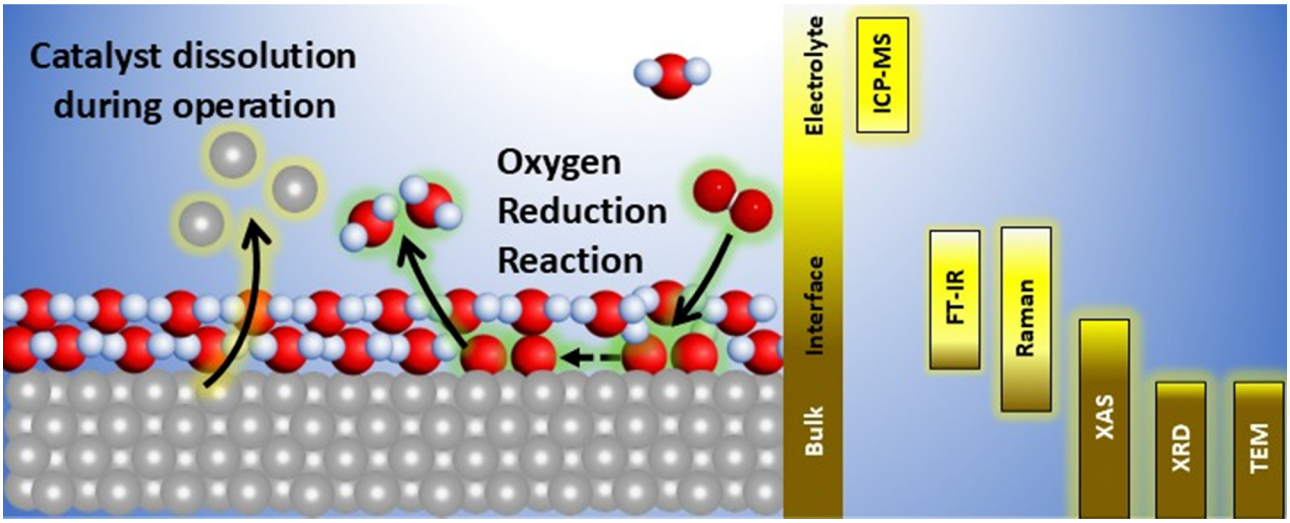

Fig. 2 Schematic representation of the electrode/electrolyte interface in electrocatalysis, and conventionally used *in situ/operando* techniques and the corresponding region probed. The oxygen reduction reaction (ORR) is sketched as example.

progress in this field, focusing on how Pt-based nanoalloys evolve in terms of their composition and structure in the earliest steps when used as ORR catalysts, which is of paramount importance when rationalizing the BoL state of ORR electrocatalysts in property–activity–stability relationships.

Pt-based nanoalloy properties during early operation steps

The use of Pt-based alloys at the nanoscale has been adopted as a reliable strategy for practical application in fuel cells since they can offer higher electrocatalytic performance than pure Pt. Ligand, strain, and ensemble effects are recognized as fundamental reactivity descriptors by which the electrocatalytic activity can be increased and activation overpotential can be reduced.[28] However, such electrocatalysts still have long-term stability challenges that must be overcome.[29] Therefore, using *in situ/operando* techniques for understanding how these nanostructures degrade is highly desirable. Although several *in situ/operando* studies can be found in the literature, systematic and detailed monitoring of the degradation of Pt-based electrocatalysts that occurs during electrode preparation and/or during the first electrochemical operation steps is seldom studied.

The first study on this topic was reported by Tuaev *et al.*,[20] who investigated the chemical and atomic-scale structural evolution of two different Pt–Ni nanostructured catalysts under electrochemical potential cycling using *in situ* anomalous small-angle X-ray scattering (ASAXS). During such activation a selective surface Ni dissolution occurs, followed by a spontaneous electrochemically induced transition from disordered alloy phases (solid solutions) to ordered Au_3Cu-type alloy structures. While core@shell structures were not formed using the Ni-richer nanoparticles ($PtNi_6$), disordered $PtNi_3$ nanoparticles formed Pt-rich core@shell structures due to the faster Ni dissolution, where compressive strain was related to the high ORR activity.

By using *in situ* X-ray diffraction, Ronovský *et al.* have recently reported that hot-pressing the membrane-electrode assembly (MEA) during preparation induces compositional changes of PtCo/C and PtNi/C electrocatalysts, revealing that dissolution is primarily driven by temperature.[30]

In another study, Gatalo *et al.*[31] have explored the effect of the applied ECA protocol on metal dissolution of a commercial Pt–Co/C and a synthesized Pt–Cu/C nanocatalyst using electrochemical online ICP-MS. The authors employed two different ECA protocols: one consisting of potential cycling (200 cycles between 0.05 and 1.2 V_{RHE} at 300 mV s^{-1}), and a second one consisting of a potential hold (0.6 V_{RHE} for 30 min). For Pt–Co/C and Pt–Cu/C nanocatalysts, both ECA protocols induced significant dissolution of Co and Cu, respectively. In the case of Pt–Cu/C, nevertheless, the potential hold protocol leads to about an order of magnitude more Cu dissolution relative to the potential cycling protocol.[31] Such Cu dissolution caused the ORR activity to diminish, which demonstrates the influence of the ECA protocol on the ORR electrocatalytic activity. Alekseenko *et al.*[32] observed dependence of ORR specific and mass activity on the upper potential limit (UPL) used in the ECA protocol by cyclic voltammetry: electrocatalysts activated by cycling in the potential range of 0.04–1.00 V_{RHE} showed 1.5–2 times higher ORR specific and mass activity compared to similar samples that were activated in the potential range from 0.04–1.20 V_{RHE}.[32] This dependence was attributed to the loss of compressive strain/ligand effect due to the Cu loss. Similar results were observed by Danisman *et al.*,[33,34] who have recently reported significant activity changes of PtNiMo/C depending on the initial ECA protocol.

In recent work, we have investigated the evolution of Pt–Nd/C nanoalloys during ECA by means of combined *operando* wide angle synchrotron X-ray scattering (WAXS)[35] and electrochemical online ICP-MS,[36] *cf.* Fig. 3. *Ex situ* characterization of the as-prepared Pt–Nd/C electrocatalyst revealed that the crystal structure corresponded to the hexagonal Pt_5Nd phase, with an induced compressive strain of approximately −3% relative to

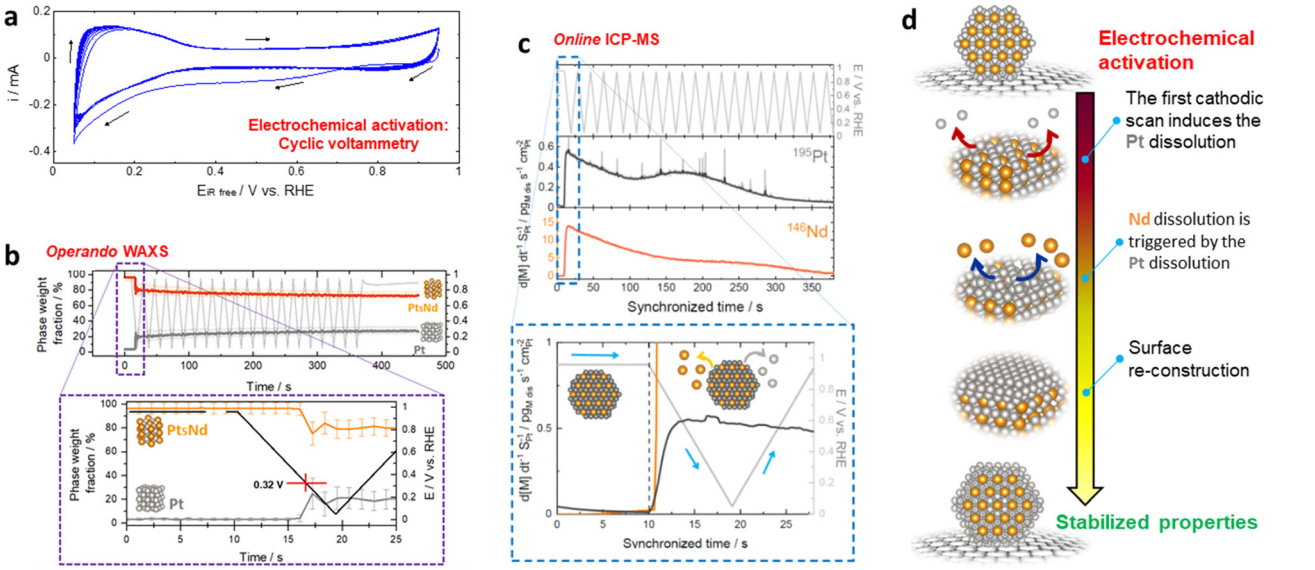

Fig. 3 Evolution of electrochemical and structural properties during electrochemical activation. (a) Electrochemical activation *via* cyclic voltammetry; (b) metallic phase weight fraction evolution, derived from refined *operando* WAXS patterns, during electrochemical activation; (c) specific dissolution profiles recorded *via* online ICP-MS during electrochemical activation of Pt–Nd/C. (d) Schematic representation of the evolution of Pt–Nd/C nanoparticles during electrochemical activation. Reproduced with permission from ref. 35 and 36 Copyright 2023, American Chemistry Society.

the Pt reference. Further, the electrocatalyst presented a core@shell structure, which comprises the Pt_5Nd alloy surrounded by a thin smooth Pt overlayer. Notwithstanding, during the ECA by cycling voltammetry (Fig. 3a), the first cathodic scan from the open circuit potential (OCP) to 0.05 V_{RHE} induced a structural modification, as observed by *operando* WAXS measurements. The refined microstructural parameters derived from the *operando* WAXS patterns (Fig. 3b) indicated a weight fraction decrease of the hexagonal Pt_5Nd phase from *ca.* 100 wt% to 80 wt%. Simultaneously, the presence of a Pt fcc component increased to 20 wt%. Both values remained almost constant on further cycling.[35] The specific dissolution profiles (Fig. 3c) indicate that the first potential transition from the OCP to 0.05 V_{RHE} induced metal dissolution, a sharp dissolution peak for Pt and Nd being observed, with the signal being stable afterwards. Interestingly, the specific dissolution profiles also revealed that Pt dissolution started slightly before that of Nd dissolution. Combining the extracted information from the *operando* WAXS and online ICP-MS experiments (see Fig. 3d), we proposed that the first potential excursion from the OCP to 0.05 V_{RHE} triggers the partial or total dissolution of the thin Pt shell produced *ex situ* by the electrochemical reduction of the already formed oxides. This Pt dissolution exposes the Nd atoms to the electrolyte, which are quickly oxidized into Nd^{3+} $E^0_{Nd^{3+}/Nd^0} = -2.323\ V_{SHE}$ that dissolve once in contact with the acidic electrolyte, thereby giving a strong thermodynamic driving force for Nd segregation from the bulk of the alloy towards the surface. This process can continue until Pt is sufficiently available to protect the Nd atoms, inducing surface reconstruction and the expected thickening of a protective Pt-rich shell, which stabilizes the surface.[36] However, the structural properties determined *ex situ* are, eventually, modified by this surface reconstruction during the conditioning step, *i.e.*, the ECA. Indeed, *in situ* XAS measurements indicated that the average local Pt–Pt interatomic distances (R_{Pt-Pt}) increased after the ECA, starting from 2.66 Å (*ex situ* measurement before ECA) to 2.67 Å (*in situ* measurement after the ECA), namely, the *ex situ* induced compressive strain is relaxed due to the surface reconstruction after the ECA, from −3.7% to −2.9%. These results clearly suggest that an overestimated *ex situ* strain magnitude might not properly rationalize the measured ORR electrochemical activity since the induced strain evolves during the activation reaction. Similar trends have been observed during the electrochemical activation of carbon-supported Pt–Y nanoalloys.[37]

In another contribution, using *in situ* IR spectroscopy and the RDE technique, Danisman *et al.*[34] have explored the number of cycles and the optimal scan rate required to achieve the first constant steady state ORR activity of trimetallic PtNiMo/C catalysts during the ECA. The authors observed that while the conventionally used fast cyclic voltammetry scans of 500 mV s^{-1} results in a lower activity (0.82 mA cm^{-2} at 0.9 V_{RHE}), a slower scan rate of 20 mV s^{-1} results in significantly higher initial activity (1.25 mA cm^{-2} at 0.9 V_{RHE}), demonstrating the important impact of the preconditioning conditions on Pt-based alloy catalysts for the ORR.

Within this context, the effect of the upper potential limit (UPL) during the ECA on the structure, chemical composition, and ORR performance of faceted Pt–Ni/C and sponge-like Pt–Ni/C nanocatalysts was studied using *operando* WAXS, electrochemical online ICP-MS and the rotating disk electrode (RDE) techniques.[23] To this end, the different Pt–Ni nanocatalysts were sequentially subjected to two electrochemical steps each one consisting in a ECA, cyclic voltammetry at 20 mV s^{-1}, and a ORR measurement. Thus, two different protocols were compared: (i) for protocol 1, the ECA was performed using

50 potential cycles at 100 mV s^{-1} in O_2-free 0.1 M $HClO_4$, with lower potential limit (LPL) and UPL respectively of 0.05 V_{RHE} and 1.0 V_{RHE}. After that, three cyclic voltammograms were acquired between 0.05–1.0 V_{RHE} at 20 mV s^{-1}. Finally, three cyclic voltammograms were acquired in the quasi-stationary state between 0.05–1.0 V_{RHE} at 5 mV s^{-1}. (ii) Protocol 2 is similar to protocol 1 with the difference of the UPL during the ECA, namely, the ECA was performed using 50 potential cycles at 500 mV s^{-1} in O_2-free 0.1 M $HClO_4$ being the LPL and UPL, respectively, 0.05 V_{RHE} and 1.23 V_{RHE}. Fig. 4 shows the acquired cyclic voltammograms, the potential-resolved lattice strain dynamics and specific metal dissolution profiles of the Pt–Ni catalysts, and those of the Pt/C benchmark. Looking at the CVs of the three materials under comparison, *cf.* Fig. 4(a)–(c), although the signals using protocol 1 and protocol 2 are reproducible, their shapes are slightly different by changing the UPL during the ECA. Namely, a potential downshift of *ca.* 30 mV on the onset of surface oxide formation is observed, which is associated with a pronounced tailing in their subsequent electrochemical reduction to a potential as low as 0.4 V_{RHE}. This feature suggests that an ECA with higher UPL leads to a more oxophilic surface in average. Interestingly, the variations of the lattice constant or electrochemical strain dynamics (derived from the *operando* WAXS patterns, Fig. 4(d)–(f)) during the cyclic voltammograms are strongly modified by the UPL during the ECA: using protocol 1 (UPL = 1 V_{RHE}) the average lattice strain presents higher degree of compression than during the protocol 2 (UPL = 1.23 V_{RHE}), which suggests a greater loss of the alloying effect benefits regarding weakened adsorption of hydrogen and oxide species. Meanwhile, the potential-resolved metal dissolution profiles, Fig. 4(g)–(l), clearly show that the electrochemical dissolution trends are affected by the UPL used during the ECA, since high metal leaching in the faceted PtNi/C using the protocol 1 is observed, which is decreased by increasing the UPL (protocol 2). Even though the trends of the sponge PtNi/C are qualitatively similar to the faceted PtNi/C, the magnitude of the metal dissolution is quantitatively lower for the former, clearly indicating that the early degradation trends depend on the catalyst structure.

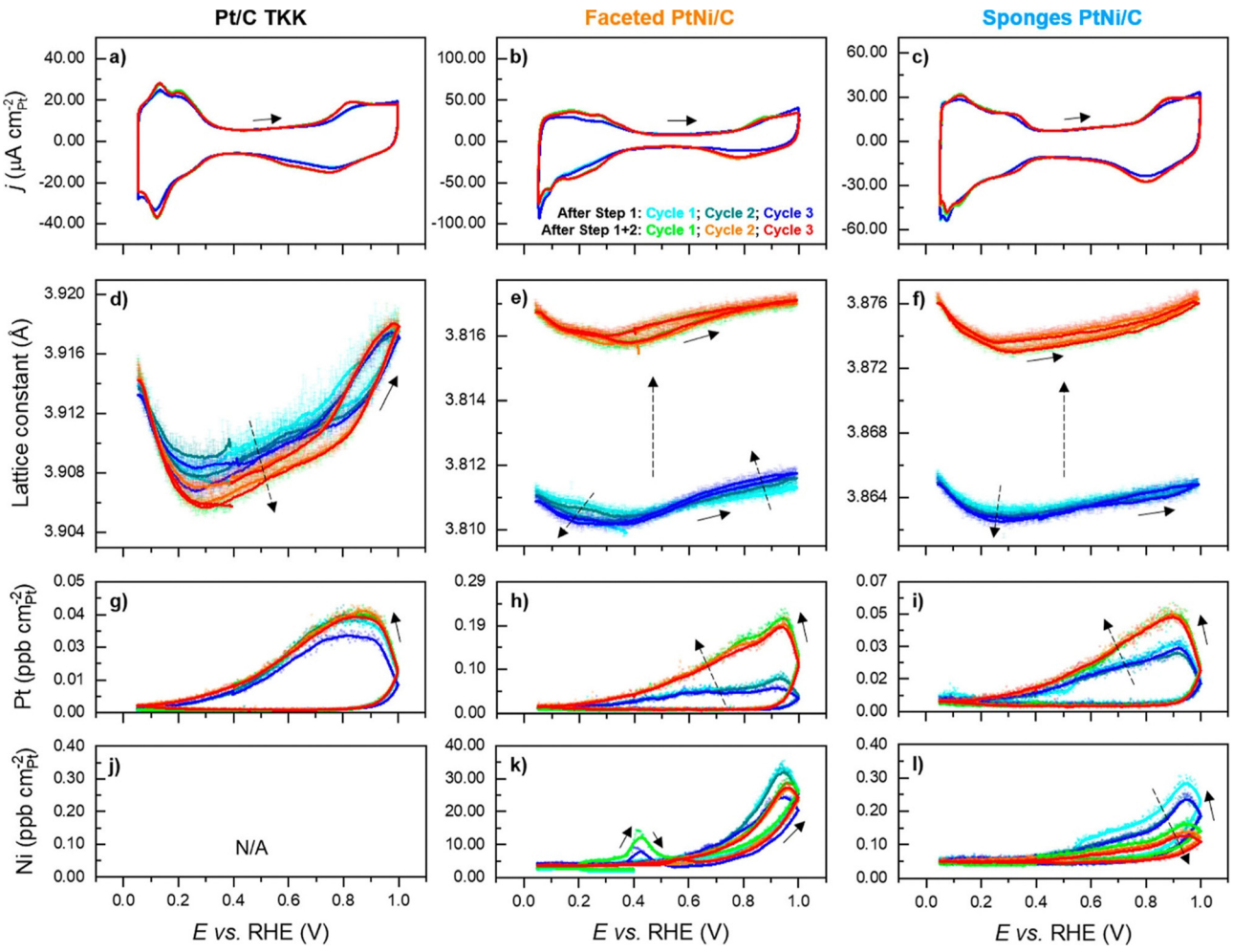

Fig. 4 (a)–(c) Cyclic voltammograms recorded at 20 mV s^{-1} using the RDE technique; (d)–(f) lattice strain dynamics measured using *operando* WAXS; specific dissolution profiles for (g)–(i) Pt and (j)–(l) Ni measured using online ICP-MS after protocol 1 (cyan, dark cyan, and blue traces) and protocol 1 + 2 (green, orange, and red traces) for Pt/C, faceted PtNi/C, and sponges PtNi/C catalysts. Reproduced with permission from ref. 23 Copyright 2022, American Chemistry Society.

In fact, by using an UPL = 1.0 V_{RHE}, activity enhancement factors (relative to the Pt/C benchmark) of 14–16 (faceted PtNi/C) and 10–11 (sponge PtNi/C) were observed; meanwhile by using an UPL = 1.23 V_{RHE} such activity enhancement factors decreased to 4–6 (faceted PtNi/C) and 8–9 (sponge PtNi/C). In conclusion, regardless of the catalyst structure, the electrochemical stabilization is accompanied by significant structural and chemical transformations for the PtNi/C nanomaterials, which eventually govern the ORR activity–stability performance.

Beyond *in situ*/*operando* measurements mimicking RDE conditions, the effect of a fast conditioning protocol by using *operando* WAXS in a single cell PEMFC (5 cm^2 MEA with a Nafion 115 membrane, targeting 0.4 mg_{Pt} cm^{-2} at the cathode, operating temperature of 80 °C and 100% relative humidity, anode and cathode sides fed with 104 sccm H_2 and 250 sccm O_2, respectively, with a 0.5 bar back pressure) was investigated using the above-discussed faceted Pt–Ni/C and sponge-like Pt–Ni/C nanocatalysts.[23] The conditioning protocol comprised five repetitions of a potential cycle of 2 min at open circuit voltage (OCV), followed by 3 min at a cell voltage of 0.85 V and 10 min at 0.65 V. The lattice expansion was measured by *operando* WAXS, relative to that of their initial structure measured by *ex situ* WAXS, after different steps of surface conditioning in a liquid cell (mimicking the RDE conditions) or in a PEMFC cell for both faceted Pt–Ni/C and sponge-like Pt–Ni/C nanocatalysts. For the faceted PtNi/C material, a lattice expansion of *ca.* 0.3% was observed to occur for the catalyst in the MEA at the very beginning of the experiment, even before the ECA was performed, this being greater than the lattice expansion observed for measurements in the liquid cell. This result suggests that the steps involved in preparing the MEA (ink formulation, sonication, deposition, hot pressing, *etc.*) led to greater catalyst degradation (equivalent to 3 Ni at% loss) than the potential cycling performed during the ECA in the liquid cell, as recently confirmed by Ronovský *et al.*[30] After the ECA of the PEMFC, the faceted PtNi/C catalyst underwent a lattice expansion of 0.45% (equivalent to a loss of 4 Ni at% from the PtNi alloy), which is more than twice that observed in the liquid cell. These observations strongly suggest that this class of shape-controlled Ni-rich catalysts are quite sensitive to the MEA preparation steps and to the PEMFC operating conditions. In the case of the sponge-like PtNi/C material, the catalyst in the MEA underwent a lattice strain relaxation of 0.16%. In fact, for this class of Ni-poor nanocatalysts, the ECA in the liquid cell and conditioning in the PEMFC both led to a lattice expansion of 0.31% (*i.e.*, 2.8% Ni at% loss).[23]

At this point and according to the discussed studies, it is clear that building up structure–activity–stability relationships using *ex situ* characterization would not *ex situ* characterization describe the nature of the true catalyst under operating conditions.

Conclusions and outlook

In this short perspective, we have highlighted the need for *in situ*/*operando* characterization of Pt-based nanoalloys during the first operation steps of the oxygen reduction reaction. Although such studies are scarce, solid evidence for the evolution of the key electrocatalytic properties (structure, chemical composition, local coordination environment, morphology, *etc.*) of Pt-based electrocatalysts during the early conditioning steps is available, which challenges the usefulness of properties measured *ex situ* as exact activity/stability descriptors in the property–activity–stability relationships.

Synchrotron-based techniques are powerful and valuable approaches for *in situ*/*operando* measurements, but lab-facility techniques, such as online ICP-MS, IR and Raman spectroscopy are also crucial in this regard. Complementary approaches including identical-location transmission-electron microscopy, machine learning-assisted theoretical calculations, and post mortem ARTEM provide further insights to the understanding of electrocatalyst properties.

Greater focus is required on the proper description of the *in situ* beginning of life catalyst state and not only on the *ex situ* catalyst state to rationalize the property–activity–stability relationships of Pt-based catalysts towards the oxygen reduction reaction,[38] including new insights at MEA level.[39] Indeed, this approach has been currently debated in the literature for oxygen evolution reaction (OER)[27,40] and CO_2 reduction reaction (CO_2RR)[41] electrocatalysts, evoking the need to understand the actual properties of any electrocatalyst for any reaction after its activation step.

Author contributions

Carlos A. Campos-Roldán: conceptualization, writing – original draft; Raphaël Chattot: conceptualization, writing – review & editing; Pierre-Yves Blanchard: supervision, writing – review & editing; Deborah J. Jones: funding acquisition, supervision, writing – review & editing; Sara Cavaliere: conceptualization, supervision, writing – review & editing.

Data availability

No primary research results, software or code have been included and no new data were generated or analysed as part of this perspective paper.

Conflicts of interest

There are no conflicts to declare.

Acknowledgements

The research leading to these results has received funding from the HIGHLANDER and IMMORTAL projects, which receive funding from the Clean Hydrogen Partnership under grant agreement numbers 101101346 and 101006641, respectively. This Joint Undertaking receives support from the European Union's Horizon Europe research and innovation programme, Hydrogen Europe, and Hydrogen Europe Research. R. C. received financial support from the French National Research Agency through the HOLYCAT project (grant no. ANR-22-CE05-0007).

References

1 M. van der Spek, C. Banet, C. Bauer, P. Gabrielli, W. Goldthorpe, M. Mazzotti, S. T. Munkejord, N. A. Røkke, N. Shah, N. Sunny, D. Sutter, J. M. Trusler and M. Gazzani, *Energy Environ. Sci.*, 2022, **15**, 1034–1077.

2 K. Kodama, T. Nagai, A. Kuwaki, R. Jinnouchi and Y. Morimoto, *Nat. Nanotechnol.*, 2021, **16**, 140–147.

3 K. Jiao, J. Xuan, Q. Du, Z. Bao, B. Xie, B. Wang, Y. Zhao, L. Fan, H. Wang, Z. Hou, S. Huo, N. P. Brandon, Y. Yin and M. D. Guiver, *Nature*, 2021, **595**, 361–369.

4 C. Y. Ahn, J. E. Park, S. Kim, O. H. Kim, W. Hwang, M. Her, S. Y. Kang, S. Park, O. J. Kwon, H. S. Park, Y. H. Cho and Y. E. Sung, *Chem. Rev.*, 2021, **121**, 15075–15140.

5 D. A. Cullen, K. C. Neyerlin, R. K. Ahluwalia, R. Mukundan, K. L. More, R. L. Borup, A. Z. Weber, D. J. Myers and A. Kusoglu, *Nat. Energy*, 2021, **6**, 462–474.

6 J. Fan, M. Chen, Z. Zhao, Z. Zhang, S. Ye, S. Xu, H. Wang and H. Li, *Nat. Energy*, 2021, **6**, 475–486.

7 C. Lee, W. J. M. Kort-Kamp, H. Yu, D. A. Cullen, B. M. Patterson, T. A. Arman, S. Komini Babu, R. Mukundan, R. L. Borup and J. S. Spendelow, *Nat. Energy*, 2023, **8**, 685–694.

8 O. M. Magnussen, J. Drnec, C. Qiu, I. Martens, J. J. Huang, R. Chattot and A. Singer, *Chem. Rev.*, 2024, **124**, 629–721.

9 J. Timoshenko and B. R. Cuenya, *Chem. Rev.*, 2021, **121**, 882–961.

10 C. A. Campos-Roldán, R. Chattot, F. Pailloux, A. Zitolo, J. Rozière, D. J. Jones and S. Cavaliere, *J. Mater. Chem. A*, 2024, **12**, 1253–1258.

11 A. A. Topalov, S. Cherevko, A. R. Zeradjanin, J. C. Meier, I. Katsounaros and K. J. J. Mayrhofer, *Chem. Sci.*, 2014, **5**, 631–638.

12 N. Hodnik, G. Dehm and K. J. Mayrhofer, *Acc. Chem. Res.*, 2016, **49**, 2015–2022.

13 T.-H. Shen, R. Girod and V. Tileli, *Acc. Chem. Res.*, 2023, **56**, 3023–3032.

14 M. Bele, G. K. Podborsek, A. Loncar, P. Jovanovic, A. Hrnjic, Z. Marinko, J. Kovac, A. K. Surca, A. R. Kamsek, G. Drazic, N. Hodnik and L. Suhadolnik, *ACS Appl. Nano Mater.*, 2023, **6**, 10421–10430.

15 A. R. Kamšek, F. Ruiz-Zepeda, A. Pavlišič, A. Hrnjić and N. Hodnik, *Curr. Opin. Electrochem.*, 2022, **35**, 101052.

16 T. Fuchs, J. Drnec, F. Calle-Vallejo, N. Stubb, D. Sandbeck, M. Ruge, S. Cherevko, D. Harrington and O. Magnussen, *Nat. Catal.*, 2020, **3**, 754–761.

17 Y. Wang, T. Gong, M. Lee and A. S. Hall, *Curr. Opin Electrochem.*, 2021, **30**, 100796.

18 M. Ma, L. Shen, Z. Zhao, P. Guo, J. Liu, B. Xu, Z. Zhang, Y. Zhang, L. Zhao and Z. Wang, *eScience*, 2024, 100254, DOI: **10.1016/j.esci.2024.100254**.

19 H. Jiang, Q. He, Y. Zhang and L. Song, *Acc. Chem. Res.*, 2018, **51**, 2968–2977.

20 X. Tuaev, S. Rudi, V. Petkov, A. Hoell and P. Strasser, *ACS Nano*, 2013, **7**, 5666–5674.

21 M. Fehse, A. Iadecola, L. Simonelli, A. Longo and L. Stievano, *Phys. Chem. Chem. Phys.*, 2021, **23**, 23445–23465.

22 M. Ronovsky, L. Pan, M. Klingenhof, I. Martens, L. Fusek, P. Kus, R. Chattot, M. Mirolo, F. Dionigi, H. Burdett, J. Sharman, P. Strasser, A. M. Bonastre and J. Drnec, *ACS Appl. Energy Mater.*, 2023, **6**, 8660–8665.

23 R. Chattot, C. Roiron, K. Kumar, V. Martin, C. A. Campos Roldan, M. Mirolo, I. Martens, L. Castanheira, A. Viola, R. Bacabe, S. Cavaliere, P.-Y. Blanchard, L. Dubau, F. Maillard and J. Drnec, *ACS Catal.*, 2022, **12**, 15675–15685.

24 J. Li and J. Gong, *Energy Environ. Sci.*, 2020, **13**, 3748–3779.

25 O. Kasian, S. Geiger, K. J. J. Mayrhofer and S. Cherevko, *Chem. Rec.*, 2019, **19**, 2130–2142.

26 K. Ehelebe, J. Knoppel, M. Bierling, B. Mayerhofer, T. Bohm, N. Kulyk, S. Thiele, K. J. J. Mayrhofer and S. Cherevko, *Angew. Chem., Int. Ed.*, 2021, **60**, 8882–8888.

27 Y. Zhu, J. Wang, H. Chu, Y.-C. Chu and H. M. Chen, *ACS Energy Lett.*, 2020, **5**, 1281–1291.

28 C. Lim, A. R. Fairhurst, B. J. Ransom, D. Haering and V. R. Stamenkovic, *ACS Catal.*, 2023, **13**, 14874–14893.

29 C. A. Campos-Roldán, D. J. Jones, J. Rozière and S. Cavaliere, *ChemCatChem*, 2022, **14**, e202200334.

30 M. Ronovský, O. Dunseath, T. Hrbek, P. Kúš, M. Gatalo, S. Polani, J. Kubát, D. Götz, H. Nedumkulam, A. Sartori, E. Petrucco, F. Ruiz-Zepeda, N. Hodnik, A. M. Bonastre, P. Strasser and J. Drnec, *ACS Energy Lett.*, 2024, **9**, 5251–5258.

31 M. Gatalo, P. Jovanovič, U. Petek, M. Šala, V. S. Šelih, F. Ruiz-Zepeda, M. Bele, N. Hodnik and M. Gaberšček, *ACS Appl. Energy Mater.*, 2019, **2**, 3131–3141.

32 A. A. Alekseenko, A. S. Pavlets, S. V. Belenov, O. I. Safronenko, I. V. Pankov and V. E. Guterman, *Appl. Surf. Sci.*, 2022, **595**, 153533.

33 B. Danisman, G. R. Zhang, A. F. Baumunk, J. Yang, O. Brummel, P. Darge, K. J. J. Mayrhofer, J. Libuda, M. Ledendecker and B. J. M. Etzold, *ChemElectroChem*, 2023, **10**, e202300109.

34 B. Danisman, G. R. Zhang, A. F. Baumunk, J. Yang, O. Brummel, P. Darge, D. Dworschak, K. J. J. Mayrhofer, J. Libuda, X. Zhou, M. Wu, E. Spiecker, M. Ledendecker and B. J. M. Etzold, *ChemElectroChem*, 2024, **11**, e202400070.

35 C. A. Campos-Roldán, R. Chattot, J.-S. Filhol, H. Guesmi, F. Pailloux, R. Bacabe, P.-Y. Blanchard, A. Zitolo, J. Drnec, D. J. Jones and S. Cavaliere, *ACS Catal.*, 2023, **13**, 7417–7427.

36 C. A. Campos-Roldán, J.-S. Filhol, H. Guesmi, M. Bigot, R. Chattot, A. Zitolo, P.-Y. Blanchard, J. Rozière, D. J. Jones and S. Cavaliere, *ACS Catal.*, 2023, **13**, 13319–13324.

37 C. A. Campos-Roldán, R. Chattot, J.-S. Filhol, H. Guesmi, N. Romero, R. Bacabe, P.-Y. Blanchard, V. Vinci, J. Drnec, J. Rozière, D. J. Jones and S. Cavaliere, *ACS Catal.*, 2024, **14**, 11941–11948.

38 A. S. Mule, K. Tran, A. M. Aleman, Y. E. Cornejo-Carrillo, G. A. Kamat, M. B. Stevens and T. F. Jaramillo, *Adv. Energy Mater.*, 2024, **14**, 2401939, DOI: **10.1002/aenm.202401939**.

39 C. A. Campos-Roldán, A. Gasmi, M. Ennaji, M. Stodel, I. Martens, J. Filhol, P. Blanchard, S. Cavaliere, D. Jones, J. Drnec and R. Chattot, *Nat. Commun.*, 2025, **16**, 936, DOI: **10.1038/s41467-024-55299-3**.

40 S. Chen, L. Ma, Z. Huang, G. Liang and C. Zhi, *Cell Rep. Phys. Sci.*, 2022, **3**, 100729.

41 W. van der Stam, *Chem. Mater.*, 2023, **35**, 386–394.